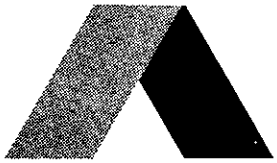

IABSE COLLOQUIUM DELFT 1987

Computational Mechanics of Concrete Structures – Advances and Applications

REPRINT FROM THE PROCEEDINGS

International Association for Bridge and Structural Engineering IABSE
Association Internationale des Ponts et Charpentes AIPC
Internationale Vereinigung für Brückenbau und Hochbau IVBH

Contact Density Model for Cracks in Concrete

Modèle de densité de contact pour les fissures dans le béton

Kontaktdichte-Modell für Risse in Beton

Baolu LI
Graduate Student
University of Tokyo
Tokyo, Japan

Baolu Li, born in 1960, received his BSc from Tongji University in China. Since 1985, he has been a graduate student of the University of Tokyo. His research interest is in the crack problems of concrete in general.

Koichi Maekawa, born in 1957, received his BSc and Dr. Eng. from the University of Tokyo. He is interested in material, structural nonlinearity and the finite element analysis of reinforced concrete.

Koichi MAEKAWA
Assoc. Professor
University of Tokyo
Tokyo, Japan

SUMMARY

A new proposal for the contact density function representing both geometrical roughness and mechanical rigidity of crack surfaces in concrete was introduced. A simple stress transfer model for cracks which is applicable to non-proportional and cyclic loading paths, was derived by combining the concept of elasto-plasticity with the proposed contact density function.

RÉSUMÉ

L'article propose une fonction de densité de contact représentant les irrégularités géométriques et la rigidité mécanique des surfaces de fissures dans le béton. Un modèle simple de transfert de contraintes pour les fissures, lequel est applicable à des systèmes de charges cycliques et non-proportionels, est dérivé en combinant le concept élasto-plastique avec la fonction de densité de contact proposée.

ZUSAMMENFASSUNG

Ein neuer Vorschlag für die Kontakt-Dichtefunktion, welche die geometrischen und mechanischen Widerstände der Rissfläche in Beton berücksichtigt, wird eingeführt. Ein einfaches Schubübertragungsmodell, das sich für statische und wiederholte Belastungen eignet, wurde abgeleitet, indem man Elasto-Plastizität mit der Kontakt-Dichtefunktion kombinierte.

1. INTRODUCTION

This paper describes the establishment of the path-dependent stress transfer model across cracks in concrete. When a shear slip δ occurs along a single crack, the resultants are the transferred shear stress τ parallel to a crack, compressive stress σ and crack opening ω normal to the crack plane. When we expect precise structural analysis by finite element methods [1], two stress components τ and σ shall be formulated under the given deformation δ and ω respectively. Many researches have been done on problems of the shear transfer in concrete crack [1,2]. However, most of the mathematical models mainly deal with so-called monotonic loading history. A simple but reasonable model of shear transfer in concrete crack taking into account of path-dependency including cyclic loading is still lacking. Without any simple and unified concepts for stress transfer, it might be very difficult to formulate the path-dependent computational model with wide applicability.

In the past, a few physical models have been proposed from a view point of crack contact surface of crack. Buyukozturk [3] represented the shape of crack surface using a simple function. Walravan [4] idealized the crack surface as a set of circular aggregates. These models simulate the stress transfer mechanism by taking into account the anisotropic crack surface geometry. On the other hand, Bazant et.al [5] introduced the microplane model assuming infinite uniaxial struts which stand on microplanes isotropically arranged in a crack band. These approaches are considered reasonable for establishing the path-dependent model, but the elasto-plastic behavior, the shear dilatancy and the direction of transferred stress under cyclic loads have not been explained by a unified concept with reasonable accuracy.

The authors introduced a contact density function representing both geometrical roughness and mechanical rigidity of crack contact surfaces in concrete. Combining the concept of elasto-plasticity with the proposed density function, a simple stress transfer model considering path-dependency including cyclic loading was proposed and computational constitutive equations were derived.

2. EFFECTIVE CONTACT DENSITY MODEL

2.1 Modeling of Crack Geometry and Stress Transfer

As illustrated in Fig.1, unit area of the crack surface was idealized as a set of infinite potential contact planes with different directional angle θ, where counterclockwise direction from y axis is defined as positive. Then the initial area of potential contact planes $dA(\theta)$, whose directions are between θ and $\theta+d\theta$, is defined by the contact density function ρ as follows.

$$dA(\theta) = A_t \rho(\theta) d\theta \qquad \int_{-\frac{\pi}{2}}^{\frac{\pi}{2}} \rho(\theta) d\theta = 1 \tag{1}$$

where, At is total area of crack surface and a constant.

Strictly speaking, the direction of contact plane and/or $\rho(\theta)$ should be a function of crack deformation (ω, δ) as shown in Fig.1. But, the crack deformation is much smaller when compared with the size of crack roughness. Therefore it can be assumed that the density function $\rho(\theta)$ is not affected by the history of crack deformation $(d\omega, d\delta)$.

Let us consider the mechanism of stress transfer. The stress (τ,σ) transferred

across a crack must be in equilibrium with total forces acting on the crack surfaces which are in contact with each other. We can define $\sigma_{con}(\theta)(>0)$ as the contact stress acting on the contact plane at the directional angle θ (See Fig.1). The stress transferred (τ,σ) can be derived as follows.

$$\tau = \int_{-\pi/2}^{\pi/2} R1(\delta,\omega,\theta)d\theta = \int A_t\, \sigma_{con}(\delta,\omega,\theta)\sin\theta_s(\delta,\omega,\theta)K(\delta,\omega,\theta)p(\theta)d\theta$$

$$\sigma = \int_{-\pi/2}^{\pi/2} R2(\delta,\omega,\theta)d\theta = \int A_t\, \sigma_{con}(\delta,\omega,\theta)\cos\theta_s(\delta,\omega,\theta)K(\delta,\omega,\theta)p(\theta)d\theta \quad (2)$$

where, σ and ω are defined as positive in compression and crack opening respectively. θs is a directional angle of contact stress acting on the negative side as defined in Fig.1. The crack opening reduces the actual contact area from the initial state. The value of K in Eq.(2) is the reduction factor and $KdA(\theta)$ is the effective contact area.

Eq.(2) is the basic constitutive equation for the proposed contact density model. The computational constitutive equations are completed when simple and appropriate functions, σ_{con}, θs, K and ρ which are mentioned above are formulated under arbitrary crack deformation paths ($d\delta$, $d\omega$).

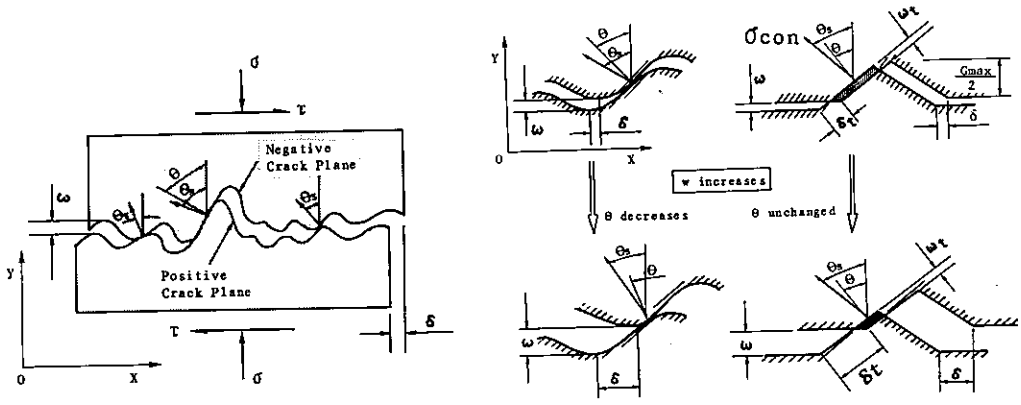

Fig.1 Idealization of Crack Contact

2.2 Mechanical Modeling

The contact stress $\sigma_{con}(\theta)$ is generated when the positive and negative planes with direction θ are met together. Hence, it may be reasonable to adopt the relative displacement parallel and normal to the contact plane as the parameters influencing the σ_{con}, θs, K and ρ.

$$\begin{aligned} \delta_t(\delta,\omega,\theta) &= \delta\cos\theta+\omega\sin\theta \\ \omega_t(\delta,\omega,\theta) &= \delta\sin\theta-\omega\cos\theta \end{aligned} \quad (3)$$

where, ωt is positive definite at closing. Increasing shear slip under the fixed crack opening causes the contact of potential planes with greater values of θ, followed by the contact of planes with smaller θ. Then, the relative

slip δt on each contact plane is observed as shown in Fig.1 or Fig.2. Because of the existence of friction, the direction of contact stress θs tilts from the normal direction of the contact plane θ. When the slip direction varies, the discontinuous change of θs occurs and results in the discontinuous rotation of transferred stress direction (τ/σ, See Fig.2). As shown in Fig.3, however, the observed stress direction under the fixed crack opening varies continuously even when the applied shear stress and slip direction are changed.
i.e.

$$\theta_s(\delta,\omega,\theta) = \theta \tag{4}$$

where, only the so-called interlock mechanism is taken into consideration. Strictly speaking, the test result shown in Fig.3 is not necessarily suitable because the slip reversal along each contact plane is not so great as to decide the micro-model of θs, but this can not be discussed further due to lack of test results. We should recognize that Eq.(4) is the approximation of the first step.

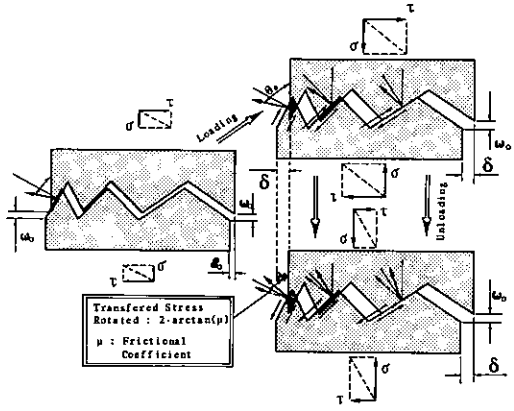

Fig.2 Direction of Contact Stress and Crack Contact Plane

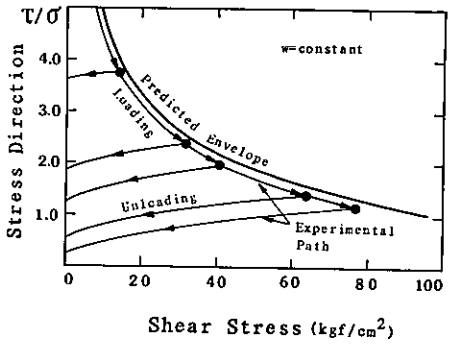

Fig.3 Direction of Stress Transfer under Cyclic Loading

When the representative roughness Gmax is idealized as shown in Fig.1, the ratio of effective contact area K is simply assumed as,

$$K(\delta,\omega,\theta) = 1 - \frac{2\,\omega}{G_{max}} \tag{5}$$

where, Gmax of normal strength concrete is the maximum size of coarse aggregate. In the case of structural analysis, the value of ω is much smaller than Gmax. Therefore the value of K is approximately equal to unity. Eq.(5) plays an important role only for extreme cases such as large crack opening or mortar.

Path-dependent and cyclic behavior of stress transfer has a close correlation with the constitutive model concerned with contact stress θcon. The total shear slip under fixed crack width (0.1~1mm) can be divided into elastic and plastic shear slip components as shown in Fig.4. But the elastic deformation has very small contribution to the total shear slip. We may adopt the most simple perfectly elasto-plastic formulation as a relationship between contact stress σcon and closing displacement ωt as shown in Fig.5.

$$\sigma_{con}(\delta,\omega,\theta) = E\,[\omega_t - \omega_{tp}] \quad , \text{ when } \omega_t > \omega_{tp} \qquad (6\text{-}1)$$
$$= 0 \quad , \text{ when } \omega_t \leqq \omega_{tp}$$

$$\omega_{tp} = \int d\omega_{tp}(\theta) \qquad (6\text{-}2)$$

$$d\omega_{tp}(\theta) = d\omega_t(\theta), \text{ if } \omega_t = \omega_{t\,max} > \omega_{lim} \text{ and } d\omega_t > 0, \text{ else}$$
$$= 0$$

where, E represents stiffness around contact planes and Wlim is the elastic limit defined as 0.004cm. The path-dependency is introduced to the model by the plastic displacement distribution $\omega_{tp}(\theta)$ in each direction, namely, $\omega_{tp}(\theta)$ memorizes the past loading history. Substituting Eq.(3)-(6) into Eq.(2), we have functions R1 and R2 concerning θ and stiffness matrix as follows.

$$R1(\delta,\omega,\theta) = m(\delta\sin\theta - \omega\cos\theta - \omega_{tp})\left(1 - \frac{2\omega}{G_{max}}\right)\sin\theta\rho(\theta)$$

$$R2(\delta,\omega,\theta) = m(\delta\sin\theta - \omega\cos\theta - \omega_{tp})\left(1 - \frac{2\omega}{G_{max}}\right)\cos\theta\rho(\theta)$$

$$\begin{Bmatrix} d\tau \\ d\sigma \end{Bmatrix} = \begin{bmatrix} D_{11} & D_{12} \\ D_{21} & D_{22} \end{bmatrix} \begin{Bmatrix} d\delta \\ d\omega \end{Bmatrix} \qquad D_{ij} = \int_{-\pi/2}^{\pi/2} \frac{\partial Ri}{\partial xi}\, d\theta \qquad (7)$$

where, m=At·E , x1=δ and x2=ω. The value of m represents the average rigidity around contact planes and is considered to be affected by the compressive strength fc'. Since the conceptual coefficient m and contact density function ρ cannot be directly determined by experiments, those values are decided by comparing the derived analytical results with experimental ones as follows (See Fig.5 and Fig.6).

$$m = 20500\, fc'^{\frac{1}{3}}$$

$$\rho(\theta) = 0.5\cos\theta \qquad (8)$$

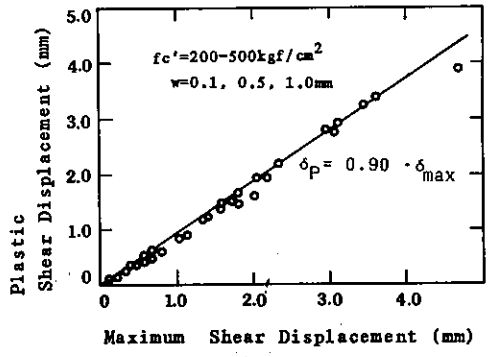

Fig.4 Plastic Shear Component

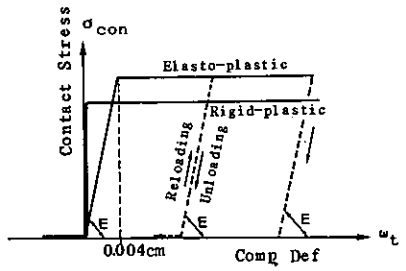

Fig.5 Model of Contact Stress.

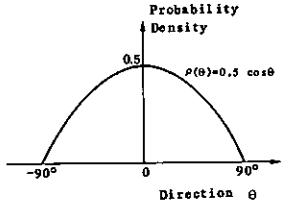

Fig.6 Model of Contact Density Function

3. EXPERIMENTAL VERIFICATION

The stress transferred across a crack is calculated by integrating R1 and R2 over the direction of θ and along a deformation path (dδ,dω) in Eq.(2). However, we must rely on the numerical integration as summarized in Appendix. The cyclic response of stress transfer under fixed crack width of 0.300mm which was obtained by authors experimentally is shown in Fig.7. Similarly, the shear transfer under various crack widths are shown in Fig.8. Using the proposed model the overall cyclic behavior of stress transfer, the shear stiffness change under various crack widths and correlation of τ and σ, that is, direction of stress transfer (τ/σ) are fairly simulated. The basic modelings regarding the plastic hysteresis of the contact stress and contact density function have a great effect on the overall response as shown in Fig.7 and Fig.8.

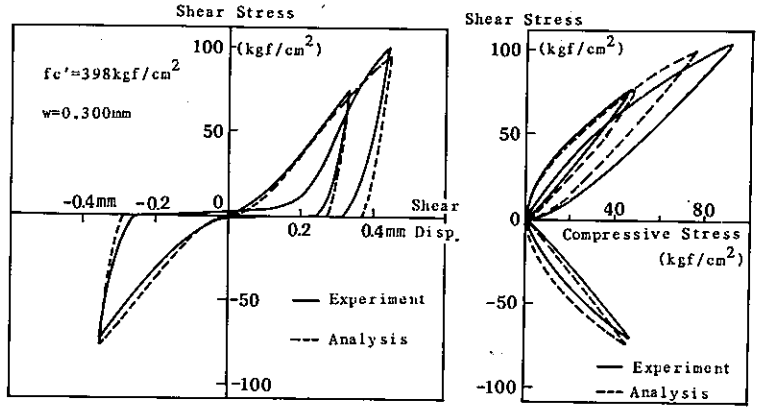

Fig.7 Cyclic Stress Transfer under Constant Crack Width

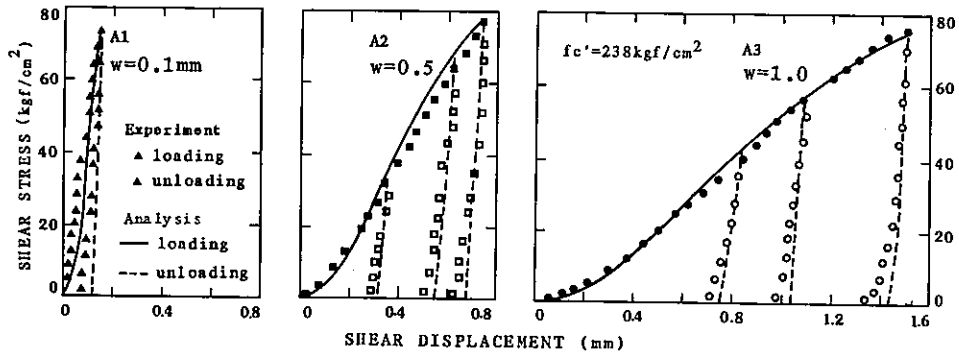

Fig.8 Shear Transfer Stiffness under Various Crack Width

In order to check the effect of loading path on the stress evaluation, the authors adopted the step type deformation paths on (δ,ω) space as shown in Fig.9(a). When shear displacement is kept constant and the crack width increases, the sustained shear stress decreases rapidly (See Fig.9(b)). When shear slip increases again under another unchanged crack width, the shear stiffness varies differently from the monotonic loading where the crack width is fixed throughout. The corresponding relation between compressive and shear stresses is shown in Fig.9(c), from which we can find the cyclic response

similar to the loading and reloading path in Fig.7. Here, the analytical model succeeds in explaining this path-dependent behavior. Path B in Fig.9(a) includes crack closing history due to increasing confining stress under a certain shear displacement. The numerically integrated solution predicts the actual response fairly (See Fig.9(d)). But compared with the monotonic loading cases, we can see the decrease in precision. The simple perfectly elasto-plastic model for contact stress may be responsible for the difference in analytical results from experimental values. Further research on more realistic cyclic model for contact stress will be necessary for the better agreement.

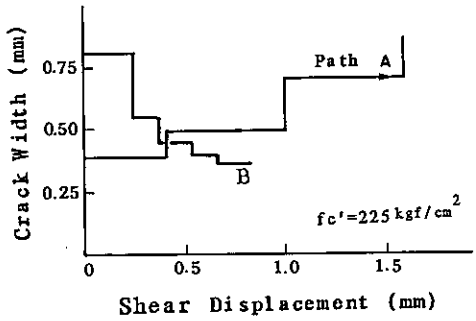

Fig.9(a) Step-type Loading path

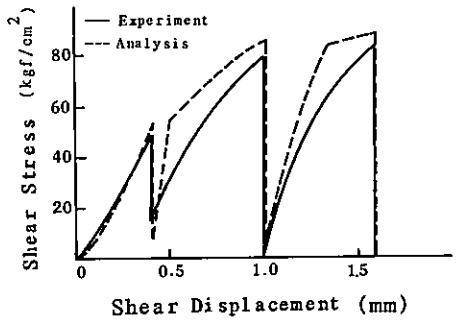

Fig.9(b) τ-δ relation of Path A

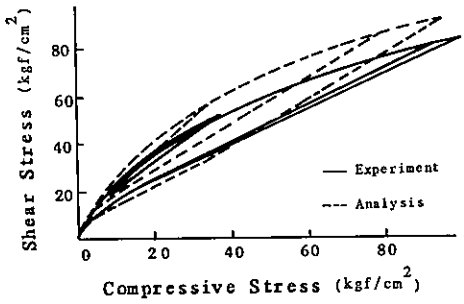

Fig.9(c) τ-σ relation of Path A

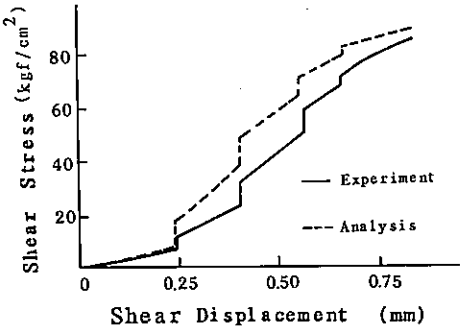

Fig.9(d) τ-δ relation of Path B

The microscopic idealization for the contact stress and density function is indirectly verified, but the effective ratio K has very small contribution to the overall behavior mentioned above, accordingly, we adopted the stress transfer across a crack in mortar as an extreme case for experimental verification. The stress transferred in mortar under constant crack width is shown in Fig.10 with analytical results, where some characteristic values of Gmax for mortar are used for trial, because we can not define the maximum size of coarse aggregate in mortar. When we select the roughness index Gmax of 1.7mm using the same functions as ρ and σcon, this model gives us fair agreement with experimental result. In other words, the crack surface condition of mortar is assumed to be represented by the similar contraction of concrete crack asperity. The same discussion holds even in the case of lightweight concrete [6].

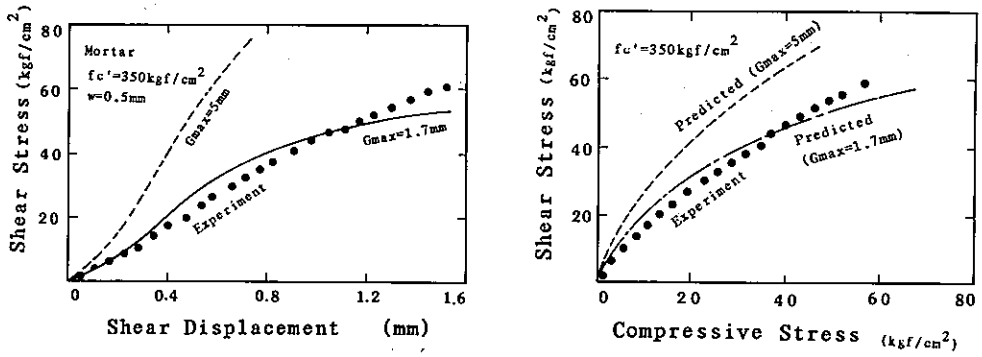

Fig.10 Stress Transfer across a Crack in Mortar

4. APPLICATION OF INTEGRATED CONSTITUTIVE EQUATIONS ON MONOTONIC LOADING

4.1 Analytical Integration and Verification

The proposed stress transfer model requires the double integral on the directional angle and deformation path, however, the analytical integration can be easily carried out on the monotonic loading path. Here, the strict definition of monotonic loading is made as the deformation path $(d\delta, d\omega)$ on which the increment of contact stress $d\sigma_{con}(\theta)$ in every direction is zero or positive. For simplicity, we assume that the rigid-plastic model for the contact stress σ_{con} neglecting the elastic component of deformation as shown in Fig.5, and that the ratio of effective contact area $K(\delta,\omega,\theta)$ is unity as discussed in Chapter 2. Accordingly, the integrands in Eq.(2) become zero when $\omega(\theta)<0$ or $-\pi/2<\theta<\tan^{-1}(\omega/\delta)$. Within the subdomain where the touch of potential contact planes occurs when $\omega(\theta)>0$, the functions R1 and R2 in Eq.(2) are converted to trigonometric functions. Using the effective domain of integration $\tan^{-1}(\omega/\delta)<\theta<\pi/2$, we have

$$\tau = k\,\frac{\delta^2}{\omega^2+\delta^2}, \qquad k = 18\,f_c'^{\frac{1}{3}} \quad (\mathrm{kgf/cm^2})$$

$$\sigma = k\left[\frac{\pi}{2} - \tan^{-1}\left(\frac{\omega}{\delta}\right) - \frac{\omega\,\delta}{\omega^2+\delta^2}\right] \tag{9}$$

Eq.(9) is a simplified particular solution of the original path-dependent constitutive model, however, it gives us exactly the same prediction as that by the original model verified by the experimental results under constant crack width (See envelopes of Fig.7 and Fig.8).

Considering actual loading paths produced in RC structures, however, the constant crack width condition used for experimental verification is not popular, but the crack width normally opens according to the increase of shear slip and/or shear stress. As an example of model verification for monotonic loading path similar to that produced in actual RC structural elements, it may be acceptable to take up a loading path with constant τ/ω, where crack width increases according to the shear loading. Relationships between $(\tau-\delta)$, $(\tau-\sigma)$ and $(\omega-\delta)$ measured from test result together with the predictions by the particular integral solution are shown in Fig.11. The shear stiffness

$(d\tau/d\delta)\tau/\omega$ decreases monotonically, not similar to the change of stiffness $(d\tau/d\delta)\omega$ under the fixed crack width, and are predicted accurately.

The simple expression shown in Eq.(9) enables us to understand the properties of the proposed original model. There exists an ultimate shear strength if a suitable confining stress is provided to keep the crack opening unchanged. This shear strength is not affected by the crack width,

$$\lim_{\delta\to\infty} \tau = \lim_{\delta\to\infty} \left[k \frac{\delta^2}{\omega^2 + \delta^2} \right] = k = 18\, fc'^{\frac{1}{3}} \qquad (10)$$

The simplified model would lose its accuracy if crack opening becomes larger, but the crack width not greater than 1mm could be considered the upper limit in general. The fact that the shear strength under fixed crack width is not affected by crack width, has also been observed experimentally by Paulay [7].

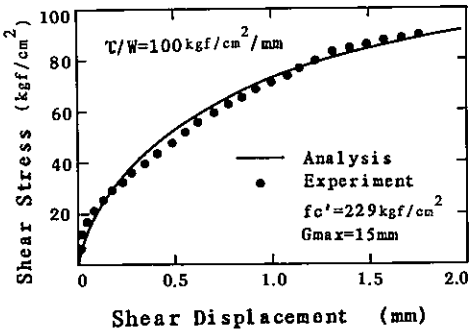

Fig.11(a) τ-δ Relation

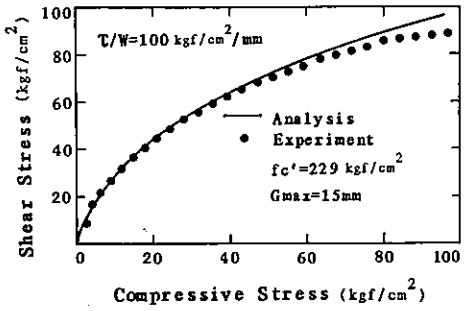

Fig.11(b) τ-σ Relation

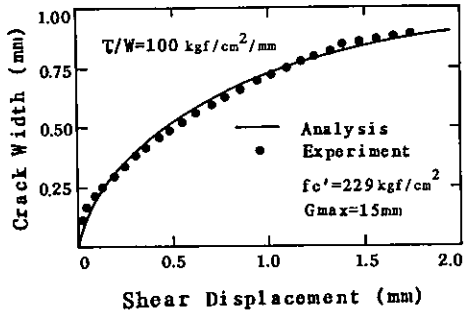

Fig.11(c) Deformational Path under Changing Crack Width Path

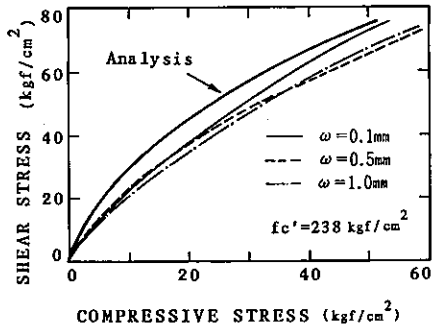

Fig.12 τ-σ Relation under Constant Crack Width

Furthermore, another interesting mechanism for the stress transfer on monotonic loading is derived from Eq.(9). Both τ and σ in Eq.(9) are functions of (ω/δ), then, we have

$$\tau = \tau(\sigma)$$

$$\text{or} \quad \sigma = \sigma(\tau) = k \left[\frac{\pi}{2} - \tan^{-1}\sqrt{\left(\frac{k}{\tau} - 1\right)} - \frac{\sqrt{\frac{k}{\tau} - 1}}{\frac{k}{\tau}} \right] \qquad (11)$$

Eq.(11) means that there exists a unique correlation between τ and σ when the plastic deformation proceeds. If crack width is kept constant, the confining stress increases with shear stress. Actually, this relation does not depend on the crack deformation (δ,ω) and can be predicted accurately by Eq.(11) as shown in Fig.12. From a view point of the theory of plasticity, we can recognize Eq.(11) as a loading function, in which stress components must satisfy when the plastic deformation flows. In the case of constant compressive stress loading path, we can observe the perfectly elasto-plastic behavior between shear stress and displacement as shown in Fig.13, where very rigid shear modulus is followed by the plastic plateau under constant shear stress. Fig.13 shows experimental loading paths and plastic flowing stress point on which crack deformations proceed rapidly. Experimentally obtained points corresponding to plastic flow coincide with the envelope given by Eq.(11) with a good accuracy.

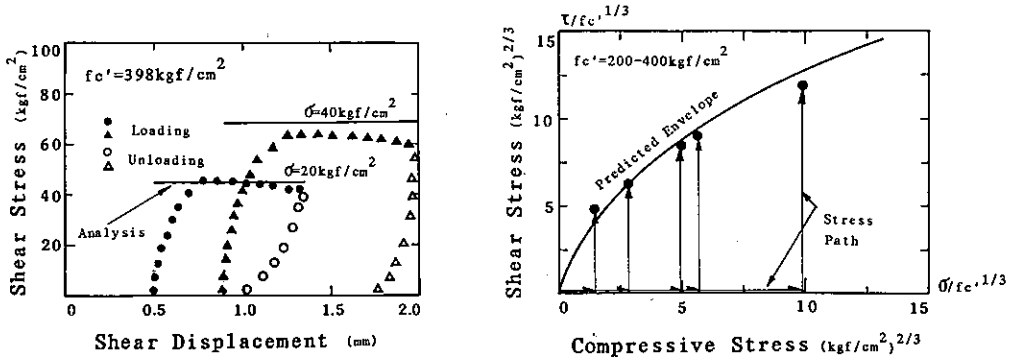

(a) (b)

Fig.13 (a) $\tau-\delta$ relation and (b) Shear Strength Under Constant Compression

4.2 Application to Smeared Crack Analysis

Let us evaluate average stiffness of an element including a number of parallel cracks. In the smeared crack procedure, the discontinuous crack deformation is considered smeared out within the total length or volume of the element considered and represented by the average strains as,

$$\gamma_{cr} = \frac{\delta}{L} \quad , \quad \varepsilon_{cr} = \frac{\omega}{L} \tag{12}$$

where, L is the characteristic length, and the average crack spacing depends on the bond characteristics between concrete and reinforcement. Substituting Eq.(12) into Eq.(9), we get

$$\tau = k \frac{\gamma_{cr}^2}{\varepsilon_{cr}^2 + \gamma_{cr}^2} \quad , \quad k = 18\, f_c'^{\frac{1}{3}} \ (kgf/cm^2)$$

$$\sigma = k \left[\frac{\pi}{2} - \tan^{-1}\left(\frac{\varepsilon_{cr}}{\gamma_{cr}}\right) - \frac{\varepsilon_{cr}\,\gamma_{cr}}{\varepsilon_{cr}^2 + \gamma_{cr}^2} \right] \tag{13}$$

where, we can find an interesting fact that the characteristic length does not appear in the above equations. This cancellation means that average stiffness of finite elements with cracks is not affected by the numbers of cracks, and is convenient for structural analysis. The authors use Eq.(13) for analysis of reinforced concrete plates subjected to in-plane loads.

5. CONCLUDING REMARKS

The path-dependent stress transfer across cracks in concrete can be simply predicted by a physical model, which is completed regarding the geometrical asperity of cracked plane by using a suitable contact distribution density function and a simple assumption of perfect elasto-plasticity in contact area. The proposed model which is capable of dealing with cyclic and non-proportional loadings was verified by experimental data. It was checked that the derived constitutive equations can be applied to structural analysis with reasonable accuracy.

The formulated constitutive equations adopt double integral along the loading path and over the contact direction, accordingly, require some numerical integration schemes in general. However, along the so-called monotonic loading path, we can easily find the particular solution derived from the original model analytically. The relationship between compressive and shear stresses acting on a crack plane is found to be mathematically unique and independent on the crack deformation under monotonic loading, and its validity was proved by experimental results.

In expanding the proposed model for a single crack to the computational model for finite elements including distributed cracks, smeared crack procedure is available whereas the characteristic length of crack spacing is generally required. However, this length affected by the bond property and other factors does not explicitly appear when we evaluate the average stiffness of elements with cracks using the integrated stress transfer model derived in this research. As a computational model, this can be applied widely.

ACKNOWLEDGMENTS

The authors are grateful to Prof.H.Okamura and Mr.J.Izumo, University of Tokyo, for their active discussion and some technical suggestions. They also would like to express their gratitude to MITUBISHI foundation and Grand-in-Aid No. 61420035 for scientific research of the Ministry of Education for providing financial support.

REFERENCES

1. State-of-the-art Report on Finite Element Analysis of Reinforced Concrete, ASCE Publication, 1984.
2. Bazant,Z.P. and Gambarova,P., "Rough Cracks in Reinforced Concrete", ST4, ASCE, Apr., 1980.
3. Fardis,M.N. and Buyukozturk,O., "Shear Transfer Model for Reinforced Concrete", ASCE, EM2, Apt., 1979.
4. Walraven,J.C. and Reinhardt,H.W., "Theory and Experiments of The Mechanical Behavior of Cracks in Plain and Reinforced Concrete Subjected to Shear Loading", Heron, Vol.26, No.1A, 1981.
5. Bazant,Z.P and Gambarava,P., "Crack shear in Concrete: Crack Bond Microplane Model", Journal of the Structural Engineering, ASCE, Vol.110, No.9, Sep., 1984.
6. Lim,T.B and Li,B.L. and Maekawa,K., "Mixed-Mode Strain-Softening Model for Shear Fracture Band on Concrete Subjected to In-plane Shear and Normal Compression", International Conference on Computational Plasticity, Spain, Apr., 1987.
7. Paulay,T. and Leober,P.J., "Shear Transfer by Aggregate Interlock", Shear in Reinforced Concrete, ACI, SP-42, Volume 1, 1974.

APPENDIX NUMERICAL INTEGRATION ALGORITHM

The stress components are obtained by conducting numerical integration of Eq.(2) with respect to directional angle θ. The following algorithm shows the accepted scheme of calculating stresses along an arbitrary crack deformation path. The crack deformation under any stress history can be easily found by the iterative calculus of Newton Raphson Method. The domain of the directional integral is divided into N pieces. The loop A in Fig.14 means the directional integral. In each direction, the plastic contact displacement ω_{tp} is determined and stored in memory, by which the path-dependency is taken into account in this model. The values of integrands R1 and R2 in Eq.(2) are stored respectively. The loop B gives the path-dependent displacement integral.

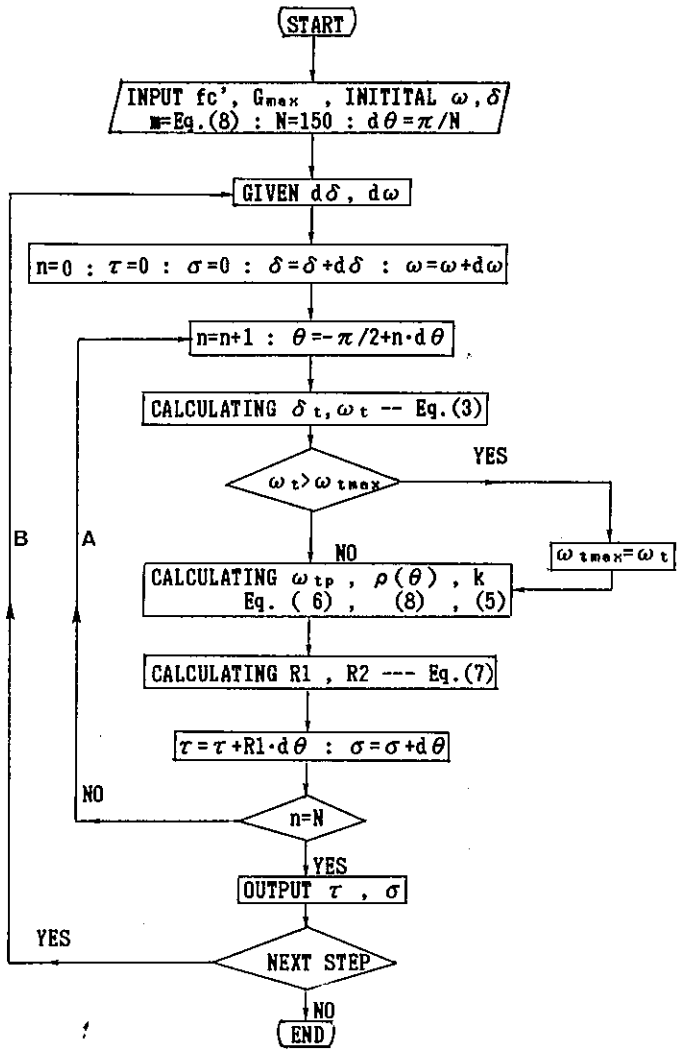

Fig.14 Numerical Integral Algorithm of Proposed Stress Transfer Model

IABSE–AIPC–IVBH

ETH-Hönggerberg
CH-8093 Zürich, Switzerland

Tel.: Int + 41 1 377 26 47
Telex: 822 186 IABS CH
Telegr.: IABSE, CH-8093 Zürich